

Effect of interfacial mobility on flexural strength and fracture toughness of glass/epoxy laminates

T. W. H. WANG, F. D. BLUM*

Department of Chemistry and Materials Research Center, University of Missouri-Rolla, Rolla, MO 65409-0010

E-mail: fblum@umr.edu

L. R. DHARANI

Department of Mechanical and Aerospace Engineering and Engineering Mechanics, University of Missouri-Rolla, Rolla, MO 65409-0050

Mechanical testing and surface fractography were used to characterize the fracture of E-glass fiber reinforced epoxy composites as a function of the silane coupling agent used. γ -Aminopropyltriethoxysilane (APS) and δ -aminobutyltriethoxysilane (ABS) were used because these have been shown to have different interfacial mobilities at multilayer coverage. The values of the properties studied generally increased from untreated <ABS- <APS-treated glass-fiber reinforced composites. Strength and critical energy release rates were more sensitive to the coupling agent used, than the modulus. The flexural strengths of untreated, ABS-, and APS-treated glass-fiber reinforced composites were 449 ± 40 , 510 ± 19 , and 566 ± 9 MPa (dry state); and 389 ± 23 , 459 ± 7 , and 510 ± 54 MPa (wet state), respectively. The critical energy release rate, G_c , as determined from a Mode I translaminar fracture toughness tests, for the untreated composites (10.5 ± 0.4 kJ/m²) was lower than that for the ABS-treated composites (14.3 ± 2.1 kJ/m²) which was lower than that for the APS-treated composites (17.1 ± 2.4 kJ/m²). Macroscopic observations showed that a larger fiber debonding area was formed in the crack tip region for the untreated glass composites, suggesting poorer bonding compared to those treated with coupling agents. Since these silanes have similar chemistry, the differences were attributed to differences in the interfacial mobility of the coupling agent layers. © 1999 Kluwer Academic Publishers

1. Introduction

Composite materials are composed of two or more components that differ in physical and chemical properties to provide specific characteristics. The boundaries between the different components are typically solid interfaces. For polymer composites, there are generally large differences between the matrix and the reinforcement in terms of density, modulus, thermal expansion, and surface energy. The most desirable properties usually can not be obtained merely through mixing and proper dispersion of raw materials.

When a polymer composite is formed, usually a fluid component in the form of a solution or melt is mixed with another component; the mixture is then solidified. The species formed at the interface would, in general, be expected to be different from the bulk materials. For example, bonding at the interface is sensitive to intermolecular or atomic forces and surface free energy. It is extremely difficult to make a quantitative determination of the mechanical properties of this interfacial portion. The characteristics of the interface are dependent on the bonding, configuration, and structure around the inter-

face, as well as the physical and chemical properties of the constituents. In order to improve the performance of composite materials, it is useful to understand the interface and the role it plays.

Generally, inorganic reinforcements have large surface energies and complicated surface structures with irregularities. The surface of inorganic reinforcements should be active both physically and chemically. Most inorganic reinforcements in common use have hydrophilic surfaces. To improve the wetting properties and dispersibility of fillers in their matrices, efforts have been under way for many years to convert hydrophilic surfaces into hydrophobic and lipophilic surfaces, based on their surface activity.

For favorable combinations of inorganic materials that have a high surface free energy and organic materials that have a low surface energy, surface treatments can be effective. Silane coupling agent treatments are widely used for inorganic materials. Zisman [1] showed that the high critical surface free energy of glass can be changed to low critical surface free energy, to a range near those of organic polymers, with various

* Author to whom all correspondence should be addressed.

silane coupling agents. A multifunctional silane coupling agent can be represented by $(RO)_3\text{-Si-R}'$, where the RO group represents a functional group which can be hydrolyzed to give a silanol group (e.g. methoxy, ethoxy), and R' may have affinity and reactivity with the matrix (e.g. vinyl, epoxy, or amino groups).

It is widely known that silane coupling agents may increase strength and rigidity in composites when used with reinforcements containing silicon [2] (e.g. glass). Some theories have been proposed to explain the behavior of silane coupling agents on the surfaces of inorganic substrates. Perhaps the most important of these are: (i) chemical reaction with the surface of the inorganic substrate to form an SiOSi bond [3] (ii) physical adsorption onto the inorganic surface [4] (iii) hydrogen bonding of the Si-OH group on the glass surface with the silanol group [5] (iv) sheathlike structures around the glass fiber [6] (v) reversible equilibrium between the hydroxyl group on the inorganic surface and the silanol group from the silane coupling agent [7].

In spite of various studies, the mechanism of these agents has not been fully clarified. Interfaces in composites are highly complicated. This complexity results from various factors, such as the methods and conditions of processing plus the type and surface condition of the inorganic substrate. Several spectroscopic techniques have been applied in the study of the interfacial properties of composites [8–12] including FT-IR, Raman, NMR and ESCA. Investigations by Ishida and Kumarends [8] using FT-IR have partially clarified the structure of silane-treated layers. Silane-treated layers do not have simple structures that allow chemical bonding on glass to form simple monomolecular layers. They form more complex stratified structures. These multilayer structures are affected by the chemical structure of the silane, the pH of the treating solution, and the surface structure of the reinforcing material.

Often the relatively small volume of the interfacial region results in it being obscured by the bulk of the reinforcement and/or polymer in spectroscopic measurements. To avoid this problem, various strategies have been explored. One way is through the use of NMR. Previous investigations from our group [13–18] using ^{29}Si CP/MAS and ^2H wide-line NMR on selectively labeled coupling agents have established that the deuterated coupling agents react with silanol sites on the surface of the substrate. These studies have given detailed information on the structure and dynamics (motional rate as well as the mechanism) of the coupling agent layer. In addition, the effects of various treatments such as overpolymerization or exposure to water were probed [18]. These studies provide the basis for understanding the molecular dynamics of the interfacial layer.

Some studies have focused on interfacial mechanical properties, especially fracture toughness of composites [19–22]. Drzal and Madhukar [19] have studied the mechanical and fracture behavior of graphite/epoxy composites by changing the level of adhesion with different surface treatments on graphite fibers. They established a relationship between the fiber/matrix interfacial shear strength and interlaminar fracture toughness for their composites. Their experimental results demonstrated

that there is a strong dependence of Mode II fracture toughness (G_{IIc}) on fiber/matrix adhesion. Increased fiber/matrix adhesion in the composites significantly improved the G_{IIc} . Studies by Drzal *et al.* [20] and Owen [21] on carbon fibers with different surface properties have highlighted the importance of the interface on composite properties. Peters and Springer [22] have shown that the mechanical properties of the composites are affected more by the fiber/matrix interface than by the degree of the cure of the matrix.

In this work, we address the relationship between the dynamics of the glass/matrix interface and the resultant flexural strength and fracture toughness of the composite. We do this by comparing composites made from glass treated with two different silane coupling agents (APS and ABS). The fracture toughness was measured in Mode I using a compact tension (CT) specimen. Flexural strength and modulus in dry and wet conditions were measured by three-point bending tests. Macroscopic and microscopic observations were employed to examine the fracture surfaces and fiber damage zones in front of crack tip.

2. Experimental

E-glass fabrics were supplied by the Owens-Corning Fiberglas Co. (Granville, OH, USA) and designated as ECG 7628 which contained 44 warps per band and 12.6 picks/cm to give a weight of 23 g/cm^2 of material. It was plain weaved to give the greatest degree of stability with respect to yarn slippage and fabric distortion. The fabrics were heat treated to remove the original sizing agents used to protect the fiber during manufacture. γ -Aminopropyltriethoxysilane (APS) was purchased from Hüls America (Piscataway, NJ, USA) and used as received. δ -Aminobutyltriethoxysilane (ABS) was prepared by hydrogenation of cyanopropyltriethoxysilane (CPS, Hüls) under a pressure of about 0.7 MPa (100 psi) and 85°C using a nickel catalyst [13]. The product was vacuum distilled at 30 mm Hg. It was then analyzed by FT-IR, ^{13}C and ^2H NMR [13].

A 2 wt% silane coupling agent solution was hydrolyzed in acetone/distilled water (10/1 weight ratio) for 24 h. The heat-cleaned glass fabrics which were cut into 15.24×15.24 cm pieces, then immersed into this solution for 24 h at room temperature. The treated glass fabrics were washed several times with distilled water and then dried in a vacuum oven at 110°C for 30 min. The amount of coupling agent deposited on the fabric could be accurately determined by thermogravimetric analysis. In principle, with the knowledge that the monolayer coverage of the coupling agent was about 4 silanols/ 100 \AA^2 [14], an equivalent thickness could be calculated. However, the uncertainty in the area available for coupling agent deposition was large because of the nature of the woven fabric. One extreme limit was that all of the glass surface on each primary fiber was available to the coupling agent, yielding an equivalent thickness of 30 layers. The other extreme limit was that the glass fabric was a flat plane; yielding the equivalent of 290 layers. A more realistic estimate was that the primary *filaments* represented the total surface area so

about 90 equivalent layers would result. In any case, it is reasonable to conclude that at similar overall coverages, both coupling agent layers had the same thickness and the amount of coupling agent used corresponded to the multilayers [23].

Epoxy resin, diglycidylether of bisphenol A (DGEBA) labelled DER331 and hardener, diethylene-triamine (DETA) labelled DEH20 were obtained from the Dow Chemical Company (Midland, MI, USA). For thorough mixing, a 10 : 1 epoxy/hardener ratio by weight was used to reach a 1 : 1 stoichiometric ratio between available hydrogen from amines and epoxy groups. The sample was well-mixed by stirring it for several minutes. Laminates were prepared by hand lay-up with 24 treated or untreated glass fabric layers in a 15.24×15.24 cm aluminum mold. It was cured in a hot press by compression molding at 115°C for 30 min with pressure of about 7 MPa. The sample was postcured at 140°C for 1 h was to insure complete curing as verified by differential scanning calorimetry.

The pressed *in situ* composites were cut into specimens 7.62 cm long and 2.54 cm wide using a band saw. The edges of the specimens were polished with 220 grit aluminum oxide sandpaper. These were tested for flexural strength and modulus as per ASTM D-0790-86 [24]. The testing was done using an Instron model 4204 testing machine at a loading rate of 0.127 cm/min. At least, 6 specimens from each sample were used. The flexural strength, S , was calculated using:

$$S = 3PL/(2bd^2) \quad (1)$$

$$f\left(\frac{a}{w}\right) = \frac{(2 + \frac{a}{w})[0.886 + 4.64(\frac{a}{w}) - 13.32(\frac{a}{w})^2 + 14.72(\frac{a}{w})^3 - 5.6(\frac{a}{w})^4]}{(1 - \frac{a}{w})^{\frac{3}{2}}} \quad (4)$$

where L is the span between the two beam supports, P is the ultimate applied load, b is the beam width, and d is the beam thickness. The flexural modulus, E , was calculated using:

$$E = mL^3/(4bd^3) \quad (2)$$

where m is the slope of the load-displacement curve. In order to get reliable data on the flexural strength, the span to depth ratio should be higher than 16 [25]. Otherwise the shear component becomes important and the flexural properties become laminate properties rather than material ones. It is also noted that the flexural properties of the translaminar configuration are governed by alignment of fabric layers [26].

The aggressive environment (wet) tests were conducted on samples which were immersed in boiling water for 2 h. Excess water was wiped off the surfaces of the samples before the testing was done.

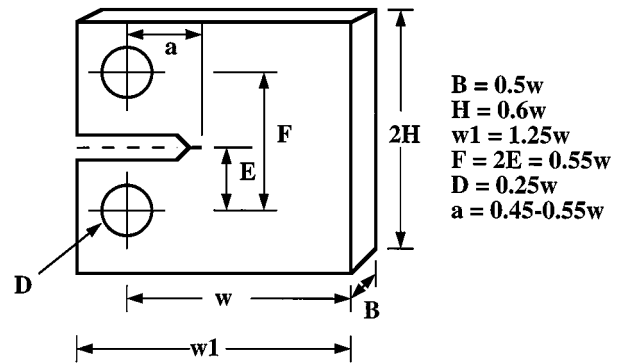


Figure 1 ASTM E833 compact tension specimen for fracture toughness. The fiber fabrics were placed in a translaminar (cross-fiber) configuration.

The geometry of a compact tension (CT) specimen is shown in Fig. 1. The specimens were shaped into ASTM E-399-83 [27] specimens with a thickness of about 0.254 cm. The precracks were cut using a diamond saw. The specimens were tested at a crosshead rate of 0.0635 cm/min. Four specimens were cut from the same batch and a total of at least eight specimens were tested for each reported value. The critical stress intensity factor (K_c) (or fracture toughness) was calculated from:

$$K_c = (P_c/Bw^{1/2})f(a/w) \quad (3)$$

where P_c is the maximum load in a loading cycle; B , w and a are denoted in Fig. 1; and $f(a/w)$ is the finite width correction [28]. For a compact tension (CT) specimen, finite width correction is:

The critical strain energy release rate, G_c , for the plane stress condition is given by:

$$G_c = K_c^2/E \quad (5)$$

where E is the modulus. For our samples, it is possible that K_c depends on the sample thickness [28] as well as other experimental variables, so a broad comparison to other work may not be appropriate. Nevertheless, since all of our specimens were made to the same thickness and measured under the same conditions, a reliable comparison among our own samples is reasonable.

Crack propagation paths were visualized on microphotographs taken by direct illumination with a Polver light microscope. The microscopic failure mode of the fracture of specimens was studied by SEM using a JEOL model JSM-35CF scanning electron microscope. Prior to the SEM observations, the specimen surfaces were coated with gold in a sputtering chamber.

TABLE I Three-point-bend test results for treated and untreated composites

	Flexural strength (MPa)		Flexural modulus (GPa)		Maximum displacement at break (cm)	
	Dry	Wet	Dry	Wet	Dry	Wet
Untreated (no postcure)	372 (5)	254 (25)	27 (1.0)	18.2 (2.5)		
Untreated (postcure)	449 (40)	389 (23)	28 (0.5)	23.6 (1.0)	0.368 (0.003)	0.363 (0.015)
ABS treated	510 (19)	459 (7)	28 (1.0)	26.0 (1.4)	0.391 (0.028)	0.373 (0.008)
APS treated	566 (9)	510 (54)	29 (1.4)	28.4 (1.7)	0.445 (0.010)	0.396 (0.043)

Uncertainties given in parentheses as 1 standard deviation.

3. Results

3.1. Load-displacement curves

Typical load-displacement curves from the three-point bend tests are shown in Fig. 2. The flexural strength, modulus, and maximum strain at break for all the composites are shown in Table I for both dry and wet samples. The untreated-glass fiber reinforced composite was first cured at 115 °C for 30 min. These samples without postcuring have the lowest flexural strength and modulus at 372 MPa and 27 GPa (dry); and 254 MPa and 18 GPa (wet), respectively. These low values were due to the incomplete cure of the resin. With postcuring at 140 °C for 1 h, the flexural strength and modulus of the composites increased to 449 MPa and 28 GPa (dry); 389 MPa and 24 GPa (wet), respectively. Composites with silane coupling-agent treated glass showed improved properties. ABS- and APS-treated composites exhibited flexural strengths of 510 and 560 MPa (dry); and 459 and 510 MPa (wet), respectively.

In all cases the strength and modulus values of the dry samples were higher than the wet ones. We note that the flexural moduli of all of the samples were similar in the dry state. The ABS- and APS-treated samples showed less of a drop in modulus when wet than those

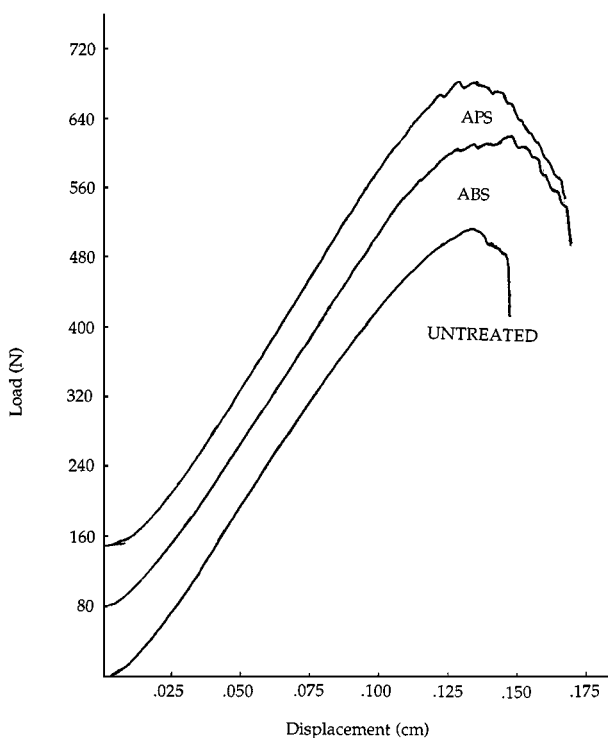


Figure 2 Typical load-displacement curves for treated and untreated composites. The vertical axis has been displaced for clarity.

of the untreated samples. A similar situation was found for the maximum displacement at break which was increased in order of untreated <ABS- <APS-treated composites.

3.2. Fracture toughness

The effect of the silane coupling agents on the critical stress intensity factor, K_{Ic} , and critical strain energy release rate, G_c , values were measured using a compact tension (CT) specimen. The values for the reinforced epoxy composites are shown in Table II. The values of K_{Ic} and G_c increased in order of untreated, ABS- and APS-treated composites which were 17, 20 and 22 (MN/m^{3/2}) for K_{Ic} , and 10.5, 14 and 17 (kJ/m²) for G_c , respectively. We note that the experimental errors for the critical strain energy release rates were quite large especially for the silane treated composites. Load-displacement curves similar to those of the three point bend tests were observed for the fracture toughness measurements. With a fixed geometry, i.e. roughly constant B and w , for all of the specimens, the differences in the stress intensity factors were chiefly dependent on P_c , the maximum load. The critical energy release rate, G_{Ic} is proportional to the stress intensity factor squared (by Equation 5). Since the modulus was roughly constant, the fracture toughness also depended mainly on the maximum load in this case. The values obtained in this study were 5–10 times higher than for unidirectional fiber reinforced epoxy composites [29], but within the same order when compared to literature values for other woven-fabric reinforced epoxy composites [30].

3.3. Macroscopic observations

A macroscopic through-thickness damage zone developed in front of the crack propagation region for each sample. Examples of these are shown in Fig. 3. At the crack tip, a blunt circular white zone was observed

TABLE II Mode I fracture toughness results of treated and untreated composites

	Critical energy release rate G_c (kJ/m ²)	Critical stress intensity factor K_{Ic} (MN/m ^{3/2})
Untreated	10.5 (0.4)	17.1 (0.2)
ABS treated	14.3 (2.1)	19.9 (1.0)
APS treated	17.1 (2.4)	22.3 (0.9)

Uncertainties given in parentheses as 1 standard deviation.

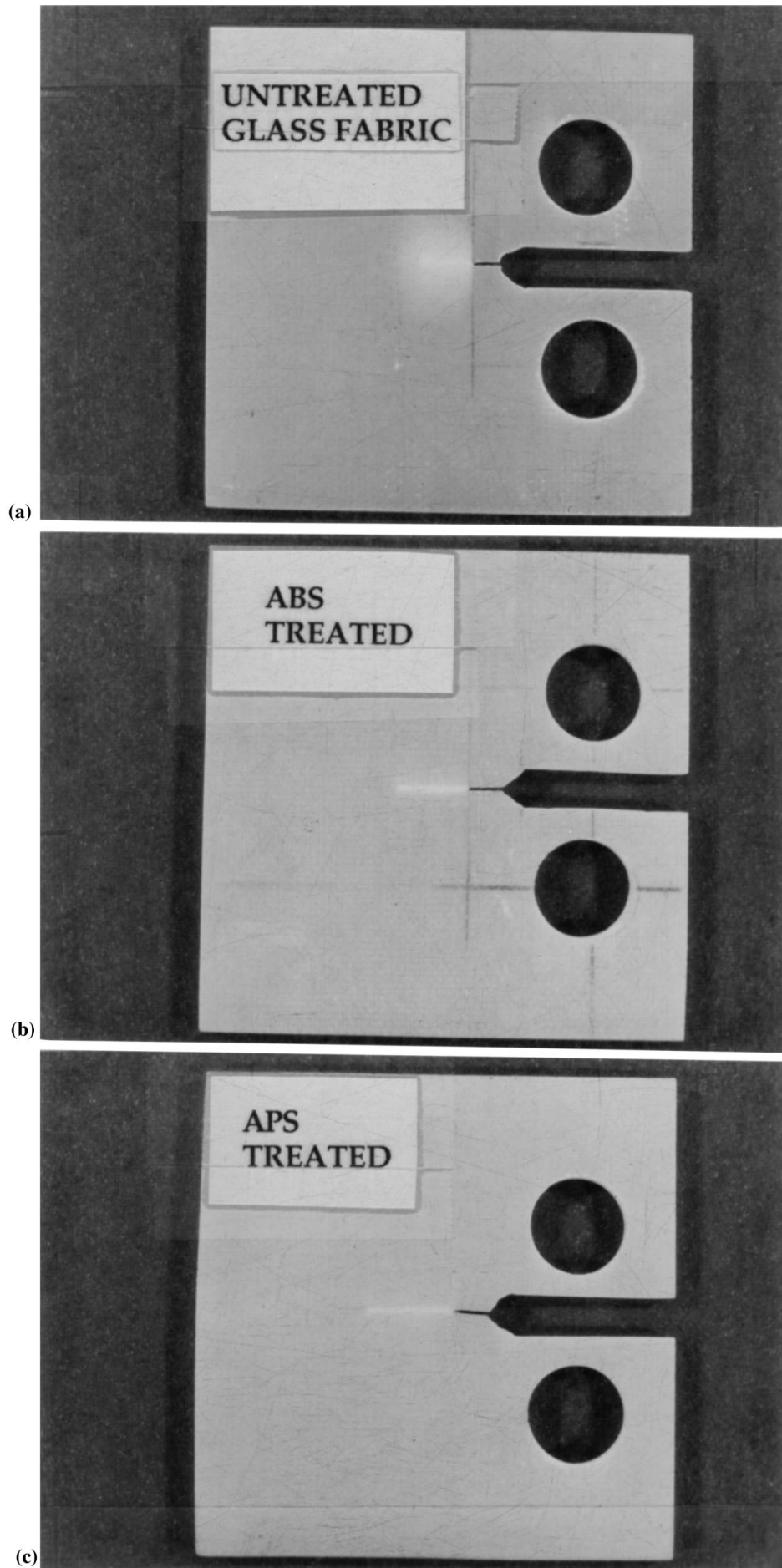


Figure 3 Visual observations of fiber fracture zones at the crack tip of the compact tension specimens for (a) untreated (b) ABS-treated and (c) APS-treated composites.

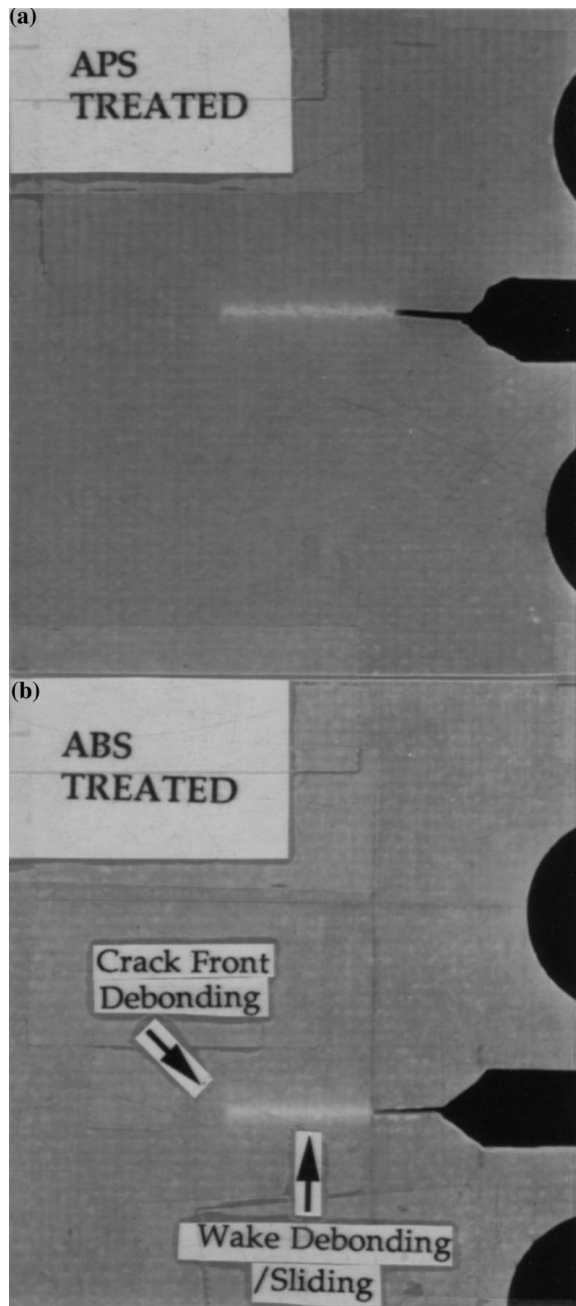


Figure 4 A closer look at the crack tip of fiber fracture zones of (a) APS-treated and (b) ABS-treated composites.

in the untreated specimen while sharp linear damage zones were observed in the silane treated specimens. The APS-treated specimens had the smallest damage zone perpendicular to the crack propagation direction. A closer look at this damage zone is shown in Fig. 4. A larger fiber debonding zone, normal to the direction of crack propagation, was observed for the ABS-treated composites than for the APS-treated ones. This difference was not large, but reproducible.

The scanning electron microscope photographs of the fracture surface of the reinforced epoxy composites from the three-point bend tests are shown in Fig. 5 (magnetization $\times 1000$). In general, the micrographs appear to be quite similar on the fracture surface between the coupling agent treated and untreated composites.

4. Discussion

The effect of the interface and its characterization have been the focus of many studies. Numerous testing methods have been employed such as, interlaminar fracture toughness tests which include Modes I, II, III and mixed, single fiber pull-out, fiber fragmentation, etc. Here, we focussed on the translaminar flexural tests and longitudinal (cross-fiber) fracture toughness of glass/epoxy composites.

4.1. Flexural properties

Kishore [31] studied translaminar flexure of glass/epoxy composites by changing the curing agent used. Plain weave E-glass fabric with epoxy-compatible silane finishes and reinforced epoxy resin was used. It was concluded that the formulation with a high temperature curing agent resulted in a greater non-linearity on modulus-strain plots in the composites. This was believed to be due to the increasing degree of fiber misalignment. Shih and Ebert [32] studied flexural failure mechanisms for unidirectional composites subjected to four-point bending tests. Using a series of coupling agents, they were able to change the interface strength and this affected the failure mode of the specimen. The apparent flexural strength decreased rapidly as the interface degraded. Bajaj *et al.* [33] investigated effects of coupling agents on the mechanical properties of mica/epoxy and glass fiber/mica/epoxy composites. Their results showed that the surface treatment of the coupling agents improved the tensile modulus, flexural strength and modulus. The property retention was also found to be better in the case of coupling-agent treated mica/epoxy composites after boiling in water for 2 h. In the case of glass-fiber/mica/epoxy composites, effects of coupling agents were not pronounced.

In the present work, the presence of either coupling agent increased the flexural strength in both dry and wet samples. This was probably due, at least in part, to the chemical bonding which occurs between the dissimilar phases. Stronger interfacial strength leads to an increase in flexural strength [32]. ABS-treated specimens had a lower flexural strength and modulus than those treated with APS. We believe that this was due to the longer alkyl chain length of ABS which did not transfer the load from the fibers to the resin as effectively as APS did. A relatively poorer interfacial region was produced.

The effect of postcure also had a measurable effect on the samples and resulted in better mechanical properties. Optimum cure conditions were not reached without postcure. This was due, in part, to unreacted epoxy/hardener with lower crosslinking density and possible voids between the fiber and matrix resin. It was also noted that the flexural strength values were approximately the same as those reported with a similar loading rate [31].

Immersion in boiling water resulted in the loss of flexural strength. For samples without coupling-agent treatment, boiling water tests revealed a larger loss in flexural strength. Water molecules have been shown [18] to migrate into interfacial regions and result in delamination of composites [2]. The flexural moduli of

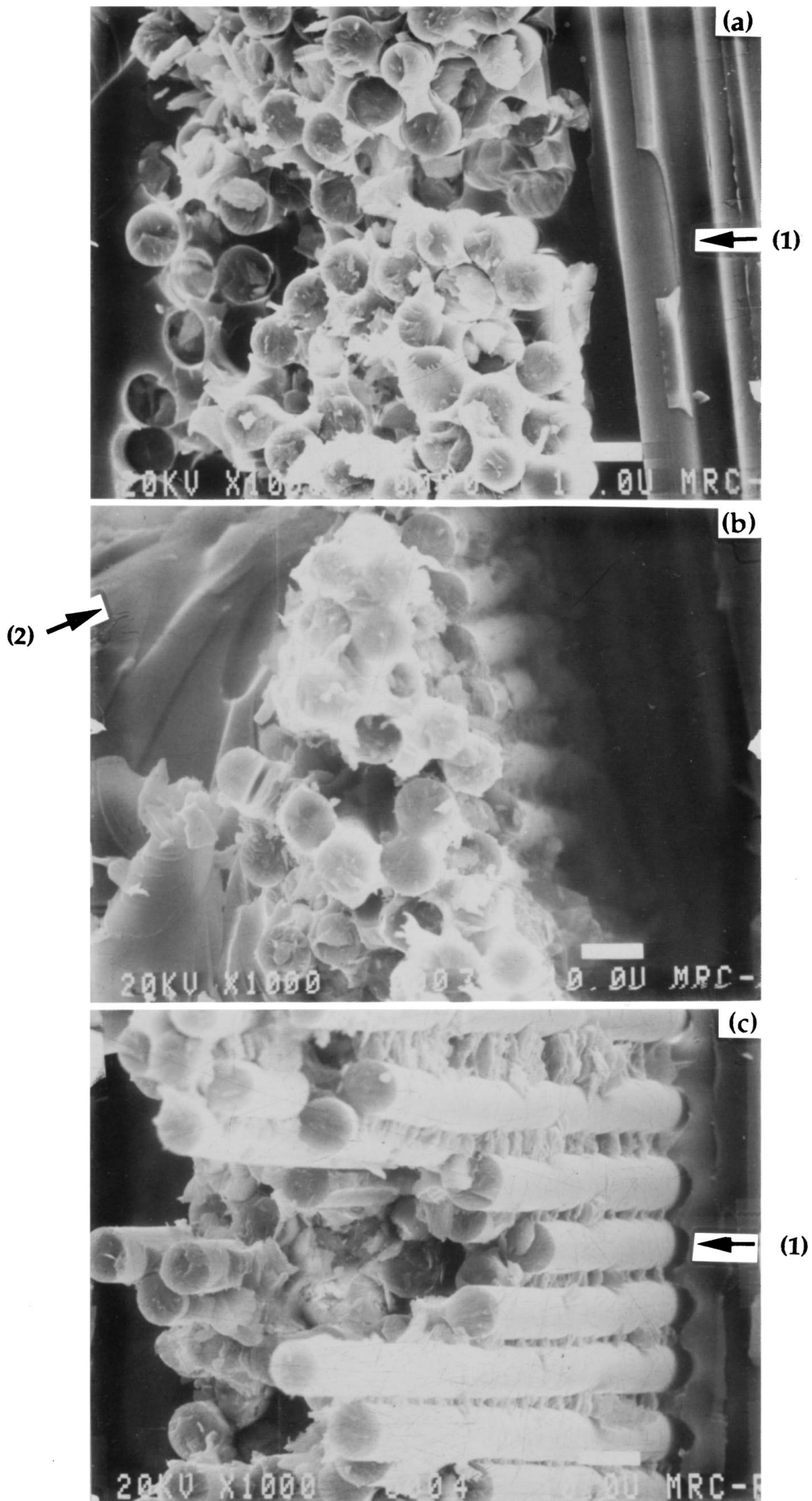


Figure 5 Scanning electron microscopic observations for the fracture surfaces of (a) untreated (b) ABS-treated and (c) APS-treated composites. Peel-like failure along transverse fibers (1) and shear cracks in resin-rich regions (2) are noted. The bars represents 10.0 μm.

all of the composites tested in the dry state were similar. Boiling water treatment did not influence the modulus of the coupling-agent treated composites, but did reduce those of the untreated composites. It is noteworthy that the flexural modulus of the ABS-treated specimens were much closer to untreated composites when dry, but were relatively better when tested wet. This suggests that even though a particular silane coupling agent was not especially effective in the dry state, it may still reduce the effect of the moisture in certain cases.

Water has been shown to have a profound effect on the molecular motion of chemisorbed coupling agents in composites [18]. Deuterium NMR line shapes of labelled coupling agents narrowed upon treatment with water and showed a rather narrow resonance when saturated with water. The narrowing of the line shape was due to increased mobility of the coupling agent in the presence of water. Upon redrying, a similar spectrum to the original sample was obtained so the interface returned more or less to its original state.

4.2. Fracture toughness

Longitudinal (cross-fiber) fracture energies were determined for the glass fiber fabric reinforced epoxy composites here using compact tension (CT) specimens. It was obvious that these tests gave much higher fracture toughness values than the interlaminar ones. Our values for the cross-fiber fracture energy for glass fabric/epoxy composites were very close to reported values [34] of about $8 \sim 11 \text{ kJ/m}^2$ for similar geometry. Some differences are expected, considering the multiple deformation mechanisms possible for a crack propagating through the fibers.

It was also reported for graphite-fiber reinforced PET matrix composites [35] that a good interfacial bond quality was achieved with a proper choice of coupling agents. Better interfacial bonding resulted in much higher K_c values than those with poor fiber/matrix adhesion. Silane coupling agents have been shown to increase the fracture toughness of composites although the effect was less profound for thermoset composites compared with thermoplastic ones [34]. A lower fracture toughness, 0.35 kJ/m^2 , was obtained when a brittle matrix was used such as unsaturated polyester than when the higher G_{1c} 0.55 kJ/m^2 , epoxy was used [30].

It is useful to compare our current results with those previously obtained by us from interlaminar fracture toughness measurements [23, 29]. It is generally true that composite materials have lower interlaminar strengths when compared with their strengths perpendicular to the fiber. It is easier for the crack to propagate parallel to, than through, the fiber. Usually, interlaminar failure initiates from regions of stress concentration, such as a free-edge, a hole or a crack and proceeds by delamination. Using mode I (double cantilever beam, DCB, specimens) interlaminar fracture toughness tests [23, 29] we found that silane coupling-agent treated composites exhibit higher critical energy release rates compared with those which were untreated. Unmodified glass-fabric reinforced epoxy composites had the average interlaminar fracture toughness of about 0.3 kJ/m^2 when compared with that of unmodified

epoxy resin [29] of about 0.1 kJ/m^2 . Clearly the geometry (interlaminar vs. longitudinal) plays a major role, but the trends relative to surface treatment are still the same.

4.3. Fractography

A fractographic analysis was carried out to understand the failure of the treated and untreated composites which revealed many interesting features of the fiber/matrix interface. It was noted that the damage zone, which appeared as a region of stress whitening on the fracture surface, had a much bigger area for untreated-glass fabric reinforced epoxy composites than the coupling-agent treated ones. The damage zone is normally a region of stable crack growth at the tip of the main crack or precut notch, consisting of subcritical cracks extending parallel to the fibers of each ply and in some cases delaminations between plies [36]. Often the size of the damage zone is closely related to the crack propagation resistance of the composites. The larger the damage zone, the higher the fracture toughness. This was not the case here. The applied stress caused massive delamination in the untreated glass composite which had the lowest fracture toughness. The size of the damage zone was also a function of the resin composition and crack tip stress distribution, e.g., bulk fracture vs. adhesive bond fracture.

The fracture patterns observed from electron microscopic studies of the three-point bend specimens could be understood, but little discrimination between the different treatments was observed. Fracture regions that included the "resin-rich" and the "fiber-rich" regions showed set patterns in the failure sequences at the interface. It was found that shear cracks were formed at an angle to the interface in the resin-rich region. These are shown in Fig. 5 where the loading direction was vertical. According to Kishore [31], matrix fracture occurs in a microscopic plane that is normal to the tensile stress. As the loading or the strain is increased, the microcracks that are formed ahead of the main crack front branch into the interface which results in curved plates of resin. However, in fiber-rich regions, hackles and scallops between two fibers positioned in the transverse direction are commonly seen. Towards the tensile face, fibers oriented parallel to the direction of crack propagation tend to form orthogonal shaped hackles in the matrix. After the separation of fiber and matrix, minuscule cusps can be seen along the fiber surfaces. These minuscule cusps, due to the shear deformation along the fiber/matrix interface after separation, were found on the silane coupling-agent treated epoxy composites. Some of these were also found in untreated composites, but the amounts were less. Peel-like failures of the resin along the transverse fibers were also present. These were due to the fiber debonding and pulling out axial fibers in the tensile face. We did not see any microflow of the resin, resin buckling, or chop marks on the compressive sides of the samples.

4.4. Interfacial mobility and its effect

Researchers have tried to relate the molecular dynamical properties with the physical properties of the

polymers [37–42]. The WLF equation [37], based on Doolittle's model [38], established a relationship between the molecular mobility and free volume of the polymers in terms of the glass transition temperature. Other physical measurements were also used to relate molecular mobility with physical properties, such as the dispersion of dielectric relaxation [39], NMR relaxation [40], diffusion of small molecules in polymers [41] and diffusion controlled aspects of crystallization and polymerization rate [42]. Recently, Parker *et al.* [43] studied the relationship between dynamic storage modulus in dynamic mechanical analysis and cross polarization rates in ^{13}C CPMAS NMR. Both the dynamic storage modulus (E') and loss modulus (E'') in the Maxwell-Weichert model were proportional to the correlation time of the materials at a specific experimental frequency. In addition, the cross polarization rates in the ^{13}C CPMAS NMR were inversely proportional to the correlation times of the polymers, thereby establishing a correlation.

Deuterium wide-line NMR techniques were also used to probe the mobility of the interfacial species in composites [13–18, 44, 45]. Results from ^2H NMR spectra for deuterated APS (DAPS) and deuterated ABS (DABS) on silica [13, 16] showed that the mobilities were a function of the alkyl chain length of the coupling agent. For a single monolayer of coupling agent, DABS and DAPS had similar mobilities. However, DABS moved considerably faster than DAPS when more than a monolayer was deposited. Subsequent studies [44, 45] in which DAPS and DABS were deposited on the silica and then reacted with epoxy and/or hardener showed that DAPS and DABS had similar line shapes at monolayer coverage, but differed substantially at the equivalent of multilayer coverage. A motional gradient appeared to exist in multilayer systems of coupling agents on silica. Since roughly 100 equivalent layers of coupling agent were deposited onto the surface, multilayers of coupling agent existed. For similar depositions of APS and ABS, we believe that this difference in mobilities between the two coupling agents played a role in the measured mechanical properties. These results suggested that ABS-treated composites have poorer interfacial properties between fiber and resin which caused the load to transfer less efficiently from resin to the fibers. Since the chemistry (reactions and interactions) of APS and ABS are similar, the differences are probably due to the differences in dynamics. Since both APS and ABS have similar behavior at the coupling agent/fiber interface (i.e. in monolayer situations), the important difference is probably due to the differences at the coupling agent/epoxy interface. The ABS/epoxy interface was inferior compared to APS/epoxy one. We propose that this was due to the molecular motion of ABS which was too fast for an optimum transition from the properties of the glass to those of the epoxy. It is postulated that APS has a better matching of physical properties at the APS/epoxy interface. Further understanding of the role of this kind of functionally graded material should allow the design of better materials.

5. Conclusions

Constant strain-rate mechanical tests provided a sensitive technique for evaluating the differences of surface treatments on glass-fabric-reinforced epoxy composites. Flexural strength, modulus and fracture toughness were influenced by the type of silane coupling agents used. Untreated composites had the lowest flexural strength and modulus which were due to a poor interface between fiber and resin. APS-treated composites had the highest flexural strength and modulus. The ABS-treated composites showed improvement over untreated glass, but not as much as for APS. The flexural moduli of the ABS- and APS-treated composites were very close to the untreated composites when tested in dry conditions, but showed substantial improvements when tested under wet conditions.

Both stress intensity factors and critical energy release rates increased in the order of untreated, ABS- and APS-treated composites. Fractographic observations of the compact tension specimens revealed that untreated composites had significantly larger damage zones, but electron microscopic pictures on the three point bend specimens did not show any significant differences. Evidence for the stronger interface in APS- and ABS-treated composites was many-fold and consistent with differences in molecular motion at the coupling agent/epoxy interface.

Acknowledgements

We gratefully acknowledge helpful discussions with Dr. P. Gopal and the financial assistance of the Office of Naval Research. We also wish to thank Mr. Robert J. Sauer of Owens-Corning Fiberglas Co. for supplying us with heat-treated fabric.

References

1. W. A. ZISMAN, *Ind Eng. Chem. Prod. Res.* **8**(12) (1969) 98.
2. E. P. PLUEDDEMANN, "Silane Coupling Agents," 2nd ed. (Plenum Press, NY, 1991).
3. H. ISHIDA and J. L. KOEING, *J. Colloid Interface Sci.* **64** (1978) 555.
4. S. WU, "Polymer Interface and Adhesion" (Marcel Dekker, New York, 1982).
5. J. G. VAIL, "Soluble Silicates" (Reinhold Publ. Co., New York, 1972) p. 171.
6. B. M. VANDERBILT, *Mod. Plast.* **37** (1959) 125.
7. H. A. CLARK and E. P. PLUEDDEMANN, *ibid.* **40** (1963) 133.
8. H. ISHIDA and G. KUMARENDAS, "Molecular Characterization of Composite Interfaces" (Plenum Press, New York, 1985) p. 25.
9. M. J. ROSEN, *J. Coatings Technol.* **50** (1978) 70.
10. K. P. HOH, I. ISHIDA and J. L. KOEING, *Annu. Tech. Conf. Soc. Plast. Eng.* **45** (1987) 1080.
11. J. P. BLITZ, M. R. S. SHREEDHARA and D. E. LEYDEN, *J. Amer. Chem. Soc.* **109** (1987) 7141.
12. J. G. MARSDEN and L. P. ZIEMIANSKI, *Br. Polym. J.* **11**(4) (1979) 199.
13. H. J. KANG, W. MEESIRI and F. D. BLUM, *Mater. Sci. Eng.* **A126** (1990) 265.
14. F. D. BLUM, W. MEESIRI, H. J. KANG and J. E. GAMBOGI, *J. Adhesion Sci. Technol.* **5** (1991) 479.
15. F. D. BLUM, *Macromol. Symp.* **84** (1994) 161.

16. H. J. KANG and F. D. BLUM, *Macromolecules* **95** (1991) 9391.
17. J. E. GAMBOGI and F. D. BLUM, *ibid.* **25** (1992) 4526.
18. *Idem.*, *Mater. Sci. Eng.* **A162** (1993) 249.
19. L. T. DRZAL and M. S. MADHUKAR, *J. Compos. Mater.* **26** (1992) 936.
20. L. T. DRZAL, M. J. RICH and S. SUBRAMONEY, in Proc. of the Third Annual Conference on Advanced Composites, Detroit, September 1987, p. 305.
21. M. J. OWEN, "Fracture and Fatigue," edited by L. J. Broutman (Academic Press, New York, 1974) p. 341.
22. P. W. M. PETERS and G. S. SPRINGER, *J. Compos. Mater.* **21** (1987) 157.
23. T. WANG and F. D. BLUM, *J. Mater. Sci.* **31** (1996) 5231.
24. "Standard Test Methods for Flexural Properties of Plastics and Electrical Insulating Materials," edited by R. P. Lukens, Annual Book of ASTM Standards (American Society for Testing and Materials, Pennsylvania, 1972).
25. C. ZWEBEN, W. S. SMITH and M. M. WARDLE, in Composite Materials: Testing and Design (5th Conference), edited by S. W. Tsai, *ASTM STP 674* (1979) 228.
26. B. GERSHON and G. MAROM, *J. Mater. Sci.* **10** (1975) 1549.
27. "Standard Test Methods for Fracture Toughness of Plastics and Electrical Insulating Materials," edited by R. P. Lukens, Annual Book of ASTM Standards (American Society for Testing and Materials, Philadelphia, Pennsylvania, 1972).
28. H. L. EWALDS and R. J. H. WANHILL, "Fracture Mechanics" (Delfts Uitgevers, Maatschappij, Netherland, 1986).
29. T. WANG and F. D. BLUM, *Polym. Prepr.* **35**(2) (1994) 755.
30. F. J. MCGARRY, in "Fundamental Aspects of Fiber Reinforced Plastic Composites," edited by R. T. Schwartz and H. S. Schwartz (Wiley Interscience, NY, 1968) p. 51.
31. K. PADMANABHAN and KISHORE, *J. Mater. Sci.* **29** (1994) 33.
32. G. C. SHIH and L. J. EBERT, *Composites* **17** (1986) 309.
33. P. BAJAJ, N. K. JHA and A. KUMAR, *J. Appl. Polym. Sci.* **44** (1992) 1921.
34. W. D. BASCOM, J. L. BITNER, R. J. MOULTON and A. R. SIEBERT, *Composites* **11** (1980) 9.
35. K. FRIEDRICH, "Fracture Mechanical Behavior of Short Fiber Reinforced Thermoplastics," Fortschrittberichte VDI, Reihe 18, Nr. 18 (VDI-Verlag, Düsseldorf, FRG, 1984).
36. J. F. MANDELL, F. J. MCGARRY, J. IM and U. MEIER, "Fiber Orientation, Crack Velocity and Cyclic Loading Effects on the Mode of Crack Extension in Fiber Reinforced Plastics," Failure Modes in Composites II, TMS/AIME, 1974.
37. J. D. FERRY, "Viscoelastic Properties of Polymers" (John Wiley, New York, 1980).
38. A. K. DOLITTLE and D. B. DOLITTLE, *J. Appl. Phys.* **28** (1957) 901.
39. W. H. STOCKMAYER, *Pure Appl. Chem.* **15** (1967) 539.
40. W. P. SLITCHER and D. D. DAVIS, *J. Appl. Phys.* **34** (1963) 98.
41. D. C. DOUGLASS and D. W. McCALL, *J. Phys. Chem.* **62** (1958) 1102.
42. J. D. GORDON and W. SIMPSON, *Polymer* **2** (1961) 383.
43. A. A. PARKER, J. J. MARCINKO, Y. T. SHIEH, D. P. HEDRIC and W. M. RITCHEY, *J. Appl. Polym. Sci.* **40** (1990) 1717.
44. T. WANG and F. D. BLUM, in Proceeding of 18th Annual Meeting (The Adhesion Society, 1995) p. 215.
45. T. WANG and F. D. BLUM, to be submitted.

*Received 4 April 1997
and accepted 9 March 1999*